CHAPTER IV
SYNTHESIS OF POLYANILINE NANOFIBRILS USING AN IN-SITU SEEDING TECHNIQUE

4.1 Abstract

Oxidative polymerization of aniline under acidic conditions, in the presence of chlorophyllin nanorods, acting as an *in-situ* seed, results in formation of nanofibrillar polyaniline (PANI). Specifically, PANI nanofibrils, with diameters in the range 60–100 nm, were formed at mole ratios of chlorophyllin to aniline monomer of 8.14×10^{-4}, 8.14×10^{-3}, and 1.63×10^{-2}; however, at a 4.07×10^{-2} mole ratio, extensive aggregation of PANI occurred. To obtain pristine PANI nanofibrils, acetone and aqueous NaOH were used as solvents to remove the chlorophyllin seed. Thus, with appropriate choice of solvent, PANI nanofibrils can be obtained in either emeraldine salt or emeraldine base forms, respectively. Analysis of the PANI nanofibrils indicates that the presence of the chlorophyllin seed during polymerization induces only a change in morphology and does not influence the molecular structure of the resulting PANI. The electrical conductivity of the pressed PANI nanofibrils is comparable to that of conventional PANI. A mechanism for the formation of PANI nanofibrils is also proposed.

4.2 Introduction

In recent years, conductive polymers synthesized in the form of nanoparticles have become of particular interest since their unique morphology, and their high specific surface area, usually result in certain advantages such as enhanced responsiveness for sensor applications (Virji, Huang, Kaner, Weiller 2004; Huang, Virji, Weiller, Kaner 2004), improved dispersion (Li, Zhao, Zhuang, Wang, Gu 2007) and a low percolation threshold for electrical conductivity in composite materials (Banerjee, Mandal 1995; Wang, Jing 2007).

Polyaniline (PANI) is one conductive polymer that has received much interest because of its facile synthesis, good environmental stability, ease of

conductivity control by changing the oxidation and protonation states, and the low cost of the monomer (Cho, Park, Hwang, Choi 2004; Zhang, Wang. 2006; Li, Gou, Wei, MacDiarmid, Lelkes 2006; Cheng, Ng, Chan 2005). In addition, PANI nanostructures have been extensively studied with respect to a wide range of applications, including sensors (Dhand, Singh, Arya, Datta, Malhotra 2007; Sadek, Wlodarski, Kalantar-Zadeh, Baker, Kaner 2007; Ajay, Divesh, Srivastava 2007; Zhu, Chang, He, Fang 2006), analytical separations (Gupta, Hellgardt, Wakeman 2006), electrorheological systems (Choi, Kim, Cho, Kim, Jhon 1997; Park, Park, Cho, Choi, Jhon 2005), and catalyst supports (Liu, Huang, Wen, Gopalan 2007). In such applications, control of the size and morphology of PANI nanostructures is generally crucial due to their strong influence on the associated properties.

Various PANI nanostructure morphologies — including tubules (Stejskal, Sapurina, Trchova, Konyushenko, Holler 2006; Wei, Kvarnstrom, Lindfors, Ivaska 2006), fibers (Wang, Jing, Kong 2007; Chiou, Epstein 2005), and spheres (Cheng, Ng, Chan 2005; Zhu, Jiang 2007) — have been synthesized by different methodologies, broadly classified into hard template and soft template techniques. Examples of the hard template method include the use of a zeolite channel (Wu, Bein 1994), a track-etched polycarbonate (Martin 1996), and an anodic aluminium oxide (AAO) (Xiong, Wang, Xia 2004). Regarding the soft template method, various species, such as surfactants (Han, Cho, Oh, Im 2002; Kim, Oh, Han, Im 2001) and polyelectrolytes (Jayanty, Prasad, Sreedhar, Radhakrishnan 2003; Sun, Park, Deng 2007), have been used as templates for the synthesis of PANI nanostructures. It is generally recognised that the hard template method might be the most effective approach to synthesize PANI nanostructures in bulk quantity with controlled particle morphology and size (Mazur, Tagowska, Palys, Jakowska 2003). However, post-processing to remove the hard template is usually required (Zhang, Wan. 2002) and such treatment run the risk of causing destruction or aggregation of the resulting PANI nanostructures, especially in cases where removal of such templates is difficult (Zhang, Wang 2006). In addition to the hard and soft template methods, synthesis of PANI nanostructures has been reported using other approaches including electrospinning (Aussawasathien, Dong, Dai 2005; Kahol, Pinto 2002), mechanical

stretching (Gu, Li, Li, Cai, Shen 2005; He, Li, Tao 2001), interfacial polymerization (He 2005; . Huang, Kaner 2004), rapid mixing polymerization (Wang, Jing 2008), sonochemical synthesis (Jing, Wang, Wu, She, Guo 2006; Jing, Wang, Wu, Qiang 2007), radiolytic synthesis (Pillalamarri, Blum, Tokuhiro, Story, Bertino. 2005), and photolithographic synthesis (Werake, Story, Bertino, Pillalamarri, Blum 2005). Zhang *et al.* (Zhang, Goux, Manohar 2004) proposed an alternative templating technique, called nanofiber seeding polymerization, for the synthesis of PANI nanofibers, in which a small amount of nanofiber, acting as the seed, produces a precipitate with fibrillar morphology. Wang *et al.* (Wang, Xu, Gong, Luo, Hou, Zheng, Qu 2005) used electrospun polyoxometalate/poly(vinyl alcohol) microfibers as a seed to synthesize PANI microrods. Microrod formation was attributed to the polymerization of aniline on the surface of the electrospun microfibers. However, the drawback of this process is the need for the pre-synthesized nanofiber seed. Subsequently, Xing *et al.* eliminated this requirement by using conventional PANI dissolved in DMSO as a seed to synthesize a nanofibrillar PANI structure (Xing, Zhao, Jing, Wang 2006).

In the present work, we describe a new approach to synthesize nanofibrillar PANI particles, using rod-like chlorophyllin, as an *in-situ* seed. Chlorophyllin is a water-soluble derivative of chlorophyll whose structure consists of a conjugated porphyrin moiety chelated around a central Cu^{II} ion (Schem. 4.1). Under acidic conditions for PANI synthesis, it was established in this study that chlorophyllin forms a nanorod-like structure and consequently serves as the *in-situ* seed for the adsorption of aniline monomer and, subsequently, polymerization of PANI on its surface. After removal of the chlorophyllin template, the resulting products exhibited homogeneous nanofibrillar morphology with a chemical structure identical to that of PANI synthesized by conventional methods (i.e. without the addition of chlorophyllin). The effect of chlorophyllin content on the formation of PANI nanofibrils and the morphology of the PANI nanostructures, isolated from the polymerization media at different time intervals, are discussed in detail. A mechanism for formation of PANI nanofibrils is proposed.

4.3 Experimental

4.3.1 Materials

The aniline monomer was purchased from Merck and purified by distillation under reduced pressure prior to use. AR grade ammoniumperoxodisulfate (APS) was also purchased from Merck. Commercial grade chlorophyllin ($C_{34}H_{31}CuN_4O_6{\cdot}3Na$; M_w = 724.1) was purchased from Aldrich. AR grade acetone, hydrochloric acid, and sodium hydroxide were purchased from Labscan and used as received.

4.3.2 Synthesis of Polyaniline Nanofibrils

PANI nanofibrils were synthesized under acidic conditions by the oxidative polymerization of aniline using APS as an oxidizing agent, in the presence of chlorophyllin acting as an *in-situ* seed. The synthesis procedure is described as follows: Chlorophyllin solutions (50 g) having four different concentrations were prepared by dissolving specific amounts of chlorophyllin — 0.05 g (0.07 mmole), 0.5 g (0.7 mmole), 1.0 g (1.4 mmole), and 2.5 g (3.5 mmole) — in distilled water. To each of the chlorophyllin solutions (50 g), 8 g (0.086 mole) of aniline monomer was added, corresponding to mole ratios of chlorophyllin to aniline monomer equal to 8.14×10^{-4}, 8.14×10^{-3}, 1.63×10^{-2}, and 4.07×10^{-2}, respectively. The mixtures were then cooled to 0°C with mechanical stirring at 300 rpm for 1 h. Next, 100 ml of 1.5 M HCl was added dropwise into each of the mixtures over a period of 30 min followed by stirring with a mechanical stirrer for 30 min. A pre-cooled solution, held at a temperature below 5°C, containing 10 g of APS (0.048 mole) in 100 ml of 1.5 M HCl was added dropwise within 30 min, after which the aniline concentration based on the total volume of the reaction mixture was 0.344 M. The reaction was stirred at 0°C for 4 h to complete the polymerization. The resulting suspension was centrifuged at 11,000 rpm for 10 min, and the obtained precipitate was re-dispersed in distilled water and dialyzed against different washing solvents including acetone, 0.5 M NaOH, and distilled water for 3 days, in order to completely remove the chlorophyllin seed. The resulting precipitate was filtered, dried under reduced pressure for 2 days, and kept in a desiccator prior to use.

4.3.3 Characterization

UV-visible spectra of the synthesized PANI were determined using a Shimadzu UV-VIS spectrometer, model 2550, in the wavelength range of 250–900 nm. A 1.5 M HCl solution and *N*-methyl-2-pyrrolidone (NMP) were used as solvents to prepare the emeraldine salt form, or doped state of PANI (PANI ES), and the emeraldine base form, or undoped state of PANI (PANI EB), respectively, at a concentration of 0.3 g/l.

FTIR spectra of the synthesized PANI were recorded using a Thermo Nicolet Nexus 670 FTIR spectrometer using the absorbance mode with 32 scans and a resolution of 4 cm^{-1}. The spectra in the frequency range of 4000–400 cm^{-1} were measured using a deuterated triglycerinesulfate detector (DTGS) with a specific detectivity of 1 x 10^9 $cm \cdot Hz^{1/2} \cdot w^{-1}$.

Morphological analysis was performed using a scanning electron microscope (JOEL, model JSM-5800LV) at 15 kV. The PANI sample was prepared by the dispersion of PANI powder in distilled water, dropped onto brass stubs and dried, followed by gold sputtering.

Thermogravimetric analysis was performed using a DuPont Instrument TGA 5.1, model 2950, over the temperature range of 30–800°C at a heating rate of 10°C/min under a nitrogen atmosphere.

X-ray diffraction (with a Rigaku, model D/MAX-2000) was carried out in continuous mode with a scan speed of 5°/min, covering angles 2θ between 5 and 50°. Cu $K\alpha_1$ was used as the X-ray source.

Electrical conductivity was measured at 25°C using a custom-made two-point probe with an electrometer/high resistance meter (Keithley, model 7517A).

4.4 Results and Discussion

4.4.1 FTIR Spectroscopy

The FTIR spectra of the acid form of the chlorophyllin seed, together with spectra of the synthesized PANI nanofibrils after removal of the chlorophyllin seed by washing with different solvents, i.e. distilled water, acetone, and a 0.5 M NaOH, are shown in Figure 4.1. In the FTIR spectrum of the PANI nanofibrils

obtained after washing with 0.5 M NaOH (Fig. 4.1d), absorption peaks were observed at 1578, 1496, 1310, and 831 cm^{-1}, assigned, respectively, to C=C stretching of the quinoid structure, C=C stretching of the benzenoid structure, C-H stretching with aromatic conjugation, and vibration of symmetrically substituted benzene. These absorption peaks are characteristic of the emeraldine base or undoped state of PANI (PANI EB) (Zhang, Wan 2002). In contrast, shifts of these peaks to lower wave numbers at 1559, 1478, 1301, and 801 cm^{-1}, respectively, were revealed in the synthesized PANI washed with distilled water and acetone, as shown in Figures 4.1b and 4.1c, respectively. This indicates the emeraldine salt or doped state of PANI (PANI ES) (Bai, Li, Li, Zuo, Wang, Li, Qiu 2007). In addition, the characteristic peaks of both undoped and doped states of the synthesized PANI nanofibrils were consistent with those of conventional PANI (data not shown). However, Figure 4.1b shows an additional characteristic peak at 1714 cm^{-1} which is assigned to the COOH stretching of residual chlorophyllin seed (see Fig. 4.1a). This suggests that washing the PANI product with distilled water does not completely remove the chlorophyllin seed owing to the poor solubility of the acid form of chlorophyllin in distilled water. In contrast, the chlorophyllin COOH stretching peak was not observed in the FTIR spectra of the PANI nanofibrillar products washed with acetone and 0.5 M NaOH solution (Figs. 4.1c and 4.1d). This result presumably reflects, respectively, the complete dissolution of the acid form of chlorophyllin in acetone, and conversion of the poorly soluble acid form of chlorophyllin to its more soluble salt form after washing with 0.5 M NaOH. Therefore, it may be concluded that acetone and 0.5 M NaOH are effective solvents for removing the chlorophyllin seed from the resulting PANI nanofibrils. Moreover, PANI with different electronic states, viz. PANI EB and PANI ES, are obtained after washing with 0.5 M NaOH and acetone, respectively. PANI EB is obtained after washing with 0.5 M NaOH because of deprotonation of PANI in the basic solvent.

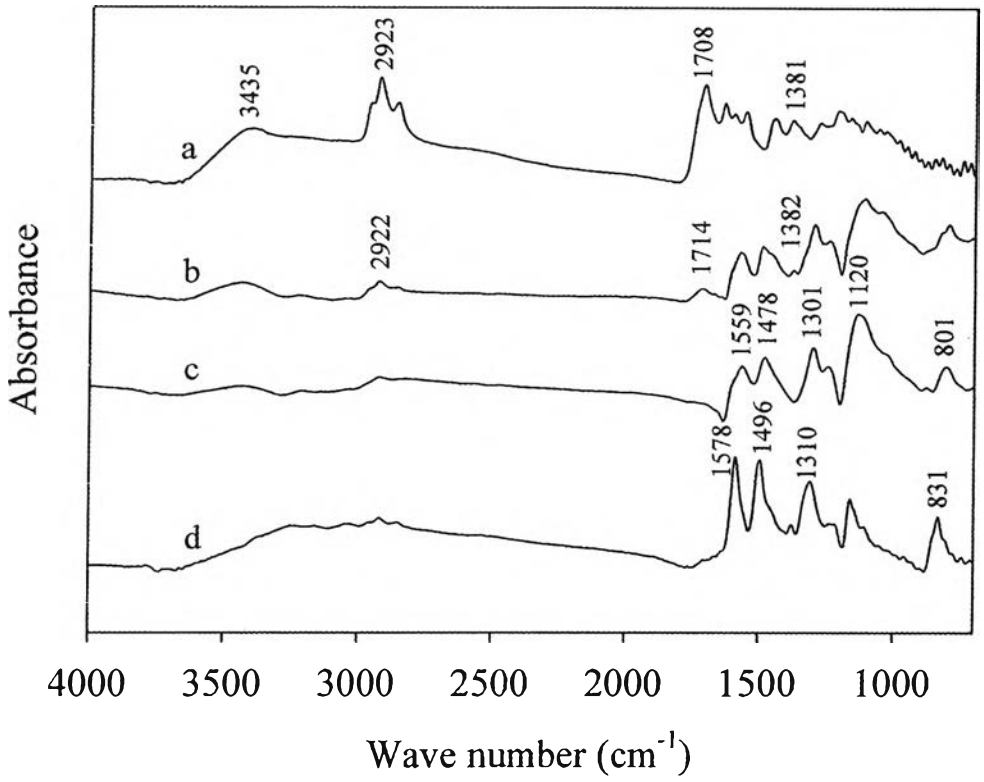

Figure 4.1 FTIR spectra of a) chlorophyllin (acid form); and PANI polymerized in the presence of 4.07×10^{-2} mole ratio of chlorophyllin to aniline monomer, after washing with b) distilled water; c) acetone; and d) 0.5 M NaOH.

4.4.2 UV-visible Spectroscopy

UV-visible spectra were used to further confirm the undoped (PANI EB) and doped (PANI ES) states of the PANI nanofibrils synthesized by the *in-situ* chlorophyllin seeding technique, as shown in Figure 4.2. A suspension of PANI nanofibrils in 1.5 M HCl exhibited absorption peaks at approximately 410 and 810 nm, which are attributed to the presence of cation radicals (polarons) and the formation of bipolarons, respectively (Xian, Liu, Feng, Wu, Wang, Jin 2007), and indicate the doped state of PANI ES. In contrast, the absorption peaks of PANI nanofibrils dissolved in NMP were shifted to 320 and 620 nm. These peaks are assigned to the π-π^* transition of the benzenoid ring and the exciton absorption of the quinoid ring, respectively (Yang, Zhao, Yu, Wei 2004; He 2005), and suggest the

undoped state of PANI EB, obtained from deprotonation of PANI in the weakly basic solvent NMP. Additionally, it was found that the UV-visible spectra of PANI nanofibrils synthesized by the *in-situ* seeding technique in both PANI ES and PANI EB forms are identical to those of PANI synthesized by the conventional method. Thus it may be concluded that the addition of the seed does not alter the electronic state of the resulting PANI products.

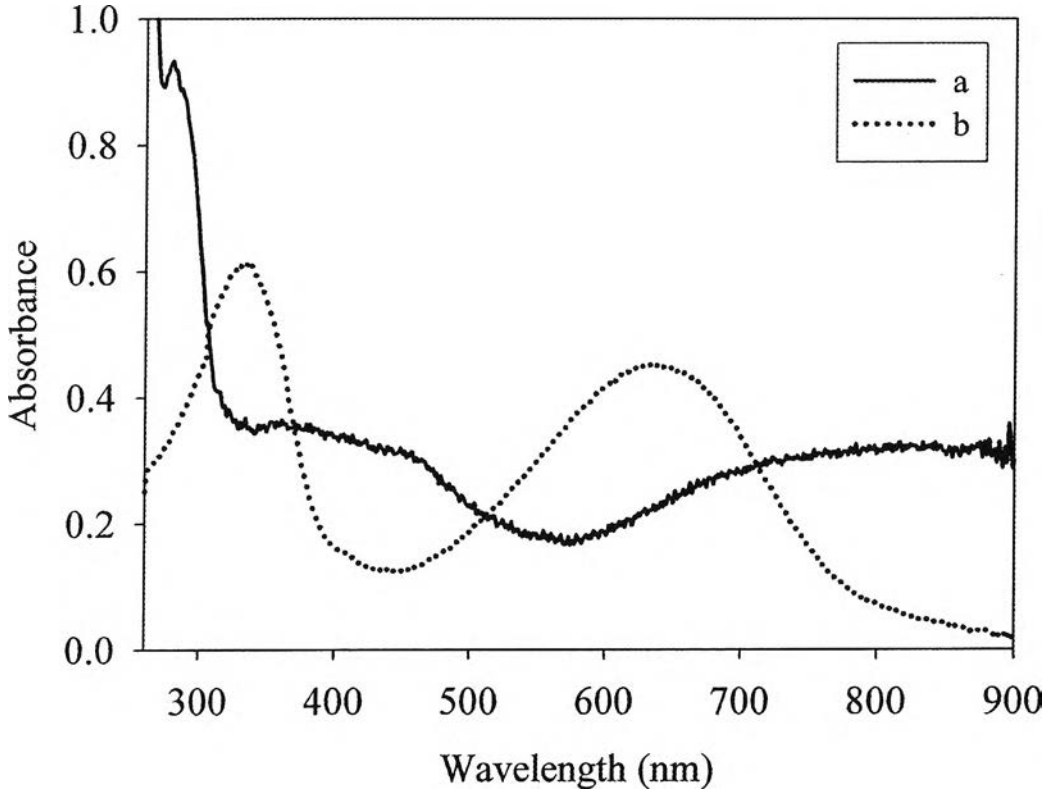

Figure 4.2 UV-visible spectra of the synthesized PANI nanofibrils: a) emeraldine salt form (PANI ES) and b) emeraldine base form (PANI EB).

4.4.3 Scanning Electron Microscopy (SEM)

Figure 4.3 shows the SEM images of the nanorod-like particles of the chlorophyllin seed (Fig. 4.3a), and compares the morphology of the PANI synthesized by the conventional method (Fig. 4.3b), versus that of the PANI nanofibrils obtained via polymerization of aniline in the presence of different chlorophyllin concentrations, after washing with acetone (Fig. 4.3c–4.3f). Figure

4.3b indicates that conventional PANI consists of irregularly-shaped PANI aggregates. Using high magnification SEM, Chiuo and Epstein (Chiou, Epstein 2005) observed that a few nanofibrils are present in the irregularly shaped PANI aggregates formed via the conventional chemical polymerization at high concentrations of aniline (~0.4 M) and APS, and, moreover, that nanofibers are predominantly formed under highly dilute conditions. Therefore, they suggest that PANI nanofibrils are intrinsically formed during the initial stages of reaction by primary nucleation and anisotropic growth. However, at high concentration of aniline, new nucleation centers are created on the primary PANI nanofibrils (secondary nucleation), resulting in formation of a branched network end eventually irregularly shaped PANI aggregates.

In contrast to the conventional polymerization, when small amounts of chlorophyllin (8.14×10^{-4}, 8.14×10^{-3}, and 1.63×10^{-2} mole ratio of chlorophyllin to aniline monomer) are added into the polymerization media (Fig. 4.3c–4.3e), it is clear that a change in morphology occurs. Specifically, uniform PANI nanofibrils with diameters in the range of 60–100 nm are formed.

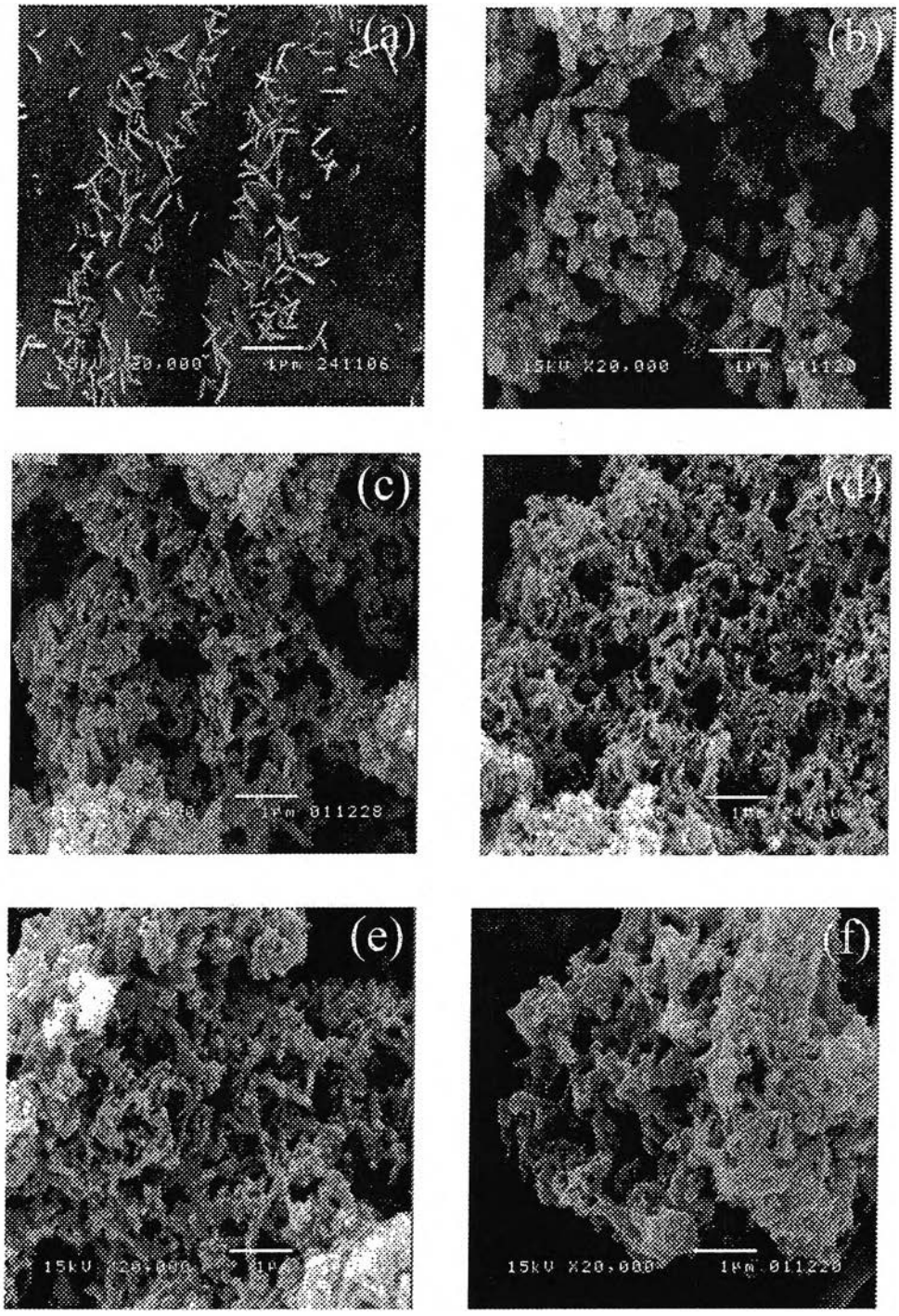

Figure 4.3 SEM images of a) nanorod-like chlorophyllin (acid form); b) conventional PANI; and PANI polymerized in the presence of different mole ratios of chlorophyllin to aniline monomer after washing with acetone: c) 8.14×10^{-4} mole ratio; d) 8.14×10^{-3} mole ratio; e) 1.63×10^{-2} mole ratio; and f) 4.07×10^{-2} mole ratio.

A possible mechanism for the formation of PANI nanofibrils using chlorophyllin as an *in-situ* seed may be proposed as follows. At high pH, chlorophyllin has three carboxylate groups (COO^-) in its structure which make the Na salt form of chlorophyllin soluble in water. Under acidic conditions, through addition of HCl, and before adding aniline monomer, the carboxylated groups of chlorophyllin become protonated (Schem. 4.1) and therefore it becomes insoluble in the polymerization medium. Under these conditions, as evident in Figure 4.3a, nanorod-like particles of chlorophyllin form with an average diameter of 57 ± 10 nm and an average length of 323 ± 47 nm. These chlorophyllin nanorods can therefore serve as the *in-situ* seeds for the adsorption and subsequent polymerization of the anilinium ion on their surfaces (Zhang, Goux, Manohar 2004). To obtain pristine PANI nanofibril products, the chlorophyllin nanorod seed particles are subsequently removed by washing with acetone, after the polymerization of anilinium ions is completed. However, as seen in Figure 4.3f, it is observed that, on increasing the chlorophyllin content up to a chlorophyllin to aniline monomer mole ratio of 4.07×10^{-2}, extensive aggregation of PANI is observed. This is may be due to aggregation of the chlorophyllin seed at higher chlorophyllin content.

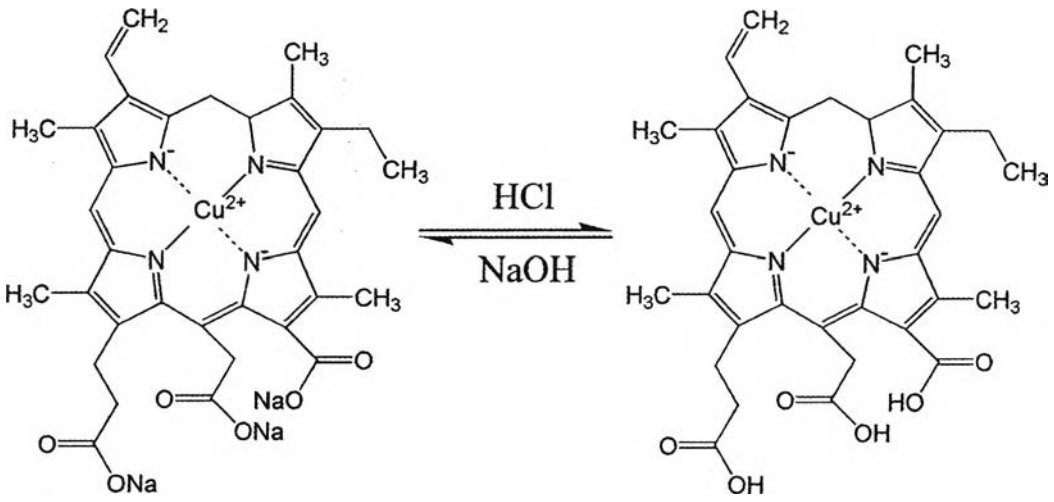

Chlorophyllin (Salt form)
(water-soluble form)

Chlorophyllin (Acid form)
(water-insoluble form)

Schematic 4.1 Chlorophyllin structures under acid–base conditions.

To gain further insight into the mechanism of formation of PANI nanofibrils by the *in-situ* seeding technique, a small quantity of PANI product was periodically collected for SEM study from the polymerization media at time intervals of 0.5, 2, and 4 h after addition of APS, the oxidizing agent. These samples were dialyzed against acetone before preparation for SEM measurement, the results of which are shown in Figure 4.4. From Figure 4.4a, agglomeration of PANI oligomers was mainly observed during the early stage of polymerization (0.5 h). However, for a longer reaction time of 2 h, polymeric PANI forms a nanofibrillar morphology (Fig. 4.4b), and, when the reaction was carried out for 4 h (Fig. 4.4c), no apparent agglomeration of PANI oligomer is observed. Based on these observations, it may be deduced that the polymerization of aniline occurs on the surfaces of the nanorod chlorophyllin seed particles. Initially, it seems possible that the anilinium ion may be adsorbed on the surface of the nanorod-like chlorophyllin seed due to electrostatic interaction and/or hydrogen bonding interactions, thus forming surface nucleation sites. Alternatively, after addition of APS, polymerization of the anilinium ion is initiated and adsorption of PANI oligomers on the seed particle surfaces may preferentially occur through hydrophobic interactions (Stejskal, Sapurina 2004; Zhang, Manohar 2004). Subsequently, anisotropic polymerization of PANI occurs along the seed surfaces to form the nanofibrillar morphology (Wang, Yang, Gong, Sui, Luo, Qu. 2006; Teoh, Liew, Mahmood 2007). From the results in Figure 4.4, it is evident that, since agglomerated PANI is isolated from the reaction mixture during the early stages of polymerization, sufficient time must be allowed for the fibrillar morphology to develop through anisotropic polymerization along the seed surfaces. Thus, it seems clear that *in-situ* chlorophyllin seed formation plays the key role in forming, stabilizing, and dispersing the PANI nanofibrils (Xing, Zhao, Jing, Wang 2006). The proposed mechanism for formation of PANI nanofibrils by *in-situ* seeding with chlorophyllin is illustrated in Schematic 4.2.

It is appropriate here to consider the possibility that the formation of PANI nanofibrils under the reaction conditions used in this study may occur without the involvement of the chlorophyllin seed particles. Specifically, we recall, as demonstrated by Chiuo and Epstein (Chiou, Epstein 2005), and confirmed by Wang *et al.* (Wang, Jing. 2008), PANI nanofibrils are formed in the conventional oxidative

polymerization of aniline by APS under dilute solution conditions (0.005 M) compared to the concentration used in the conventional method ~0.4 M. Under these circumstances, the formation of PANI nanofibrils has been attributed to the reduced number of secondary nucleation sites on surface of the primary PANI nanofibrils (Chiou, Epstein 2005; Wang, Jing. 2008). Also, Zhang *et al.* have proposed that the formation of nanofibrillar PANI in dilute solution conditions results from the rod-like structure of anilinium-peroxodisulfate ion clusters, formed during the induction period, which act as *in-situ* generated seed particles (Zhang, Kolla, Wang, Raja, Manohar 2006). We do not consider such mechanisms are relevant in our work in view of the relatively high concentration of aniline in the reaction mixture (0.344 M).

It is pertinent here to point out that, while PANI nanofibrils can be formed intrinsically under dilute solution conditions (0.005 M) without introducing seed particles, the potential of such methods for scale-up to produce PANI nanofibrils in large quantity is limited, requiring use of a large-volume reactor as well as a large volume of the reaction medium. In the present work, a small amount of chlorophyllin seed is added to the polymerization media to serve as the seed for the adsorption and subsequent polymerization of the anilinium ion. Moreover, since evidently the presence of chlorophyllin seed suppresses or prevents secondary nucleation on the primary PANI nanofibrils, the method works with high concentrations of aniline and APS, and therefore, may be effectively used to scale up the reaction to produce large quantities of PANI nanofibrils over a broad range of aniline concentrations.

From our discussion above, it should be clear that complete removal of the chlorophyllin seed is a key factor, since residual chlorophyllin may affect the useful properties of the resulting PANI, most importantly the electrical properties (Guo, Zhou 2007). Figure 4.5 shows the SEM images of PANI nanofibrils washed with different types of solvents, i.e. acetone, 0.5 M NaOH, and distilled water. It was found that the PANI products after washing with acetone and 0.5 M NaOH solution had clearly fibrillar morphology (Figs. 4.5a and 4.5b). In addition, the evidence from FTIR spectra (see Figs 4.1c and 4.1d) also indicates the absence of the COOH group belonging to the chlorophyllin seed. Therefore, acetone and 0.5 M NaOH solution may be considered as effective solvents for removing the chlorophyllin seed.

Moreover, the PANI nanofibrils obtained after washing with 0.5 M NaOH are in the emeraldine base form (PANI EB) owing to deprotonation of PANI. In addition, PANI nanofibrils containing some agglomeration of the chlorophyllin seed were observed when water was used as a washing solvent, as shown in Figure 4.5c. This suggests only partial removal of the chlorophyllin seed by distilled water. Since the acid form of chlorophyllin is only partially dissolved in water due to its lower polarity, compared to the salt form, some chlorophyllin seed remains in the resulting PANI nanofibrils. Residual chlorophyllin seed is also evidenced by FTIR spectral analysis (see Fig. 4.1b).

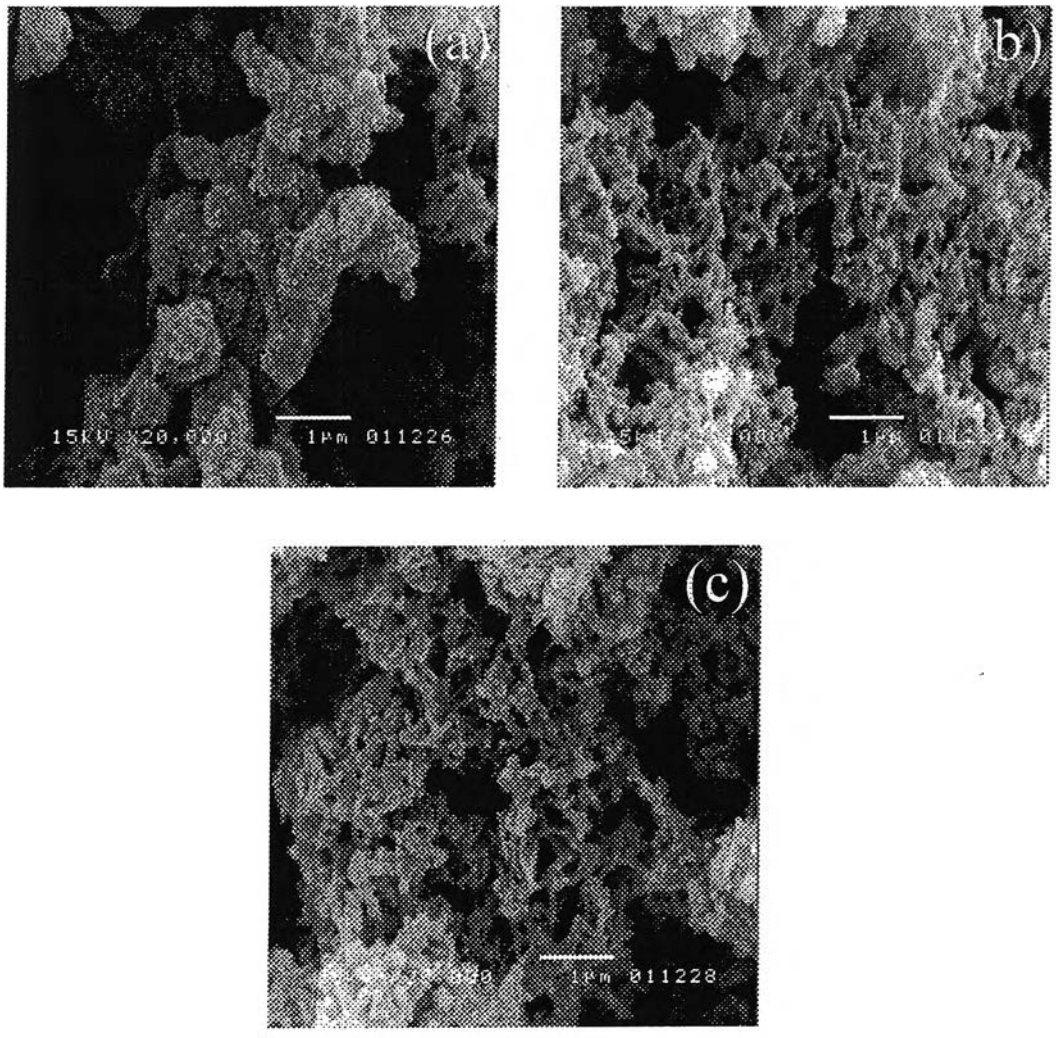

Figure 4.4 SEM images of PANI polymerized in the presence of 8.14×10^{-4} mole ratio of chlorophyllin to aniline monomer, isolated from the polymerization reaction at different reaction times: a) 0.5 h; b) 2 h; and c) 4 h, after washing with acetone.

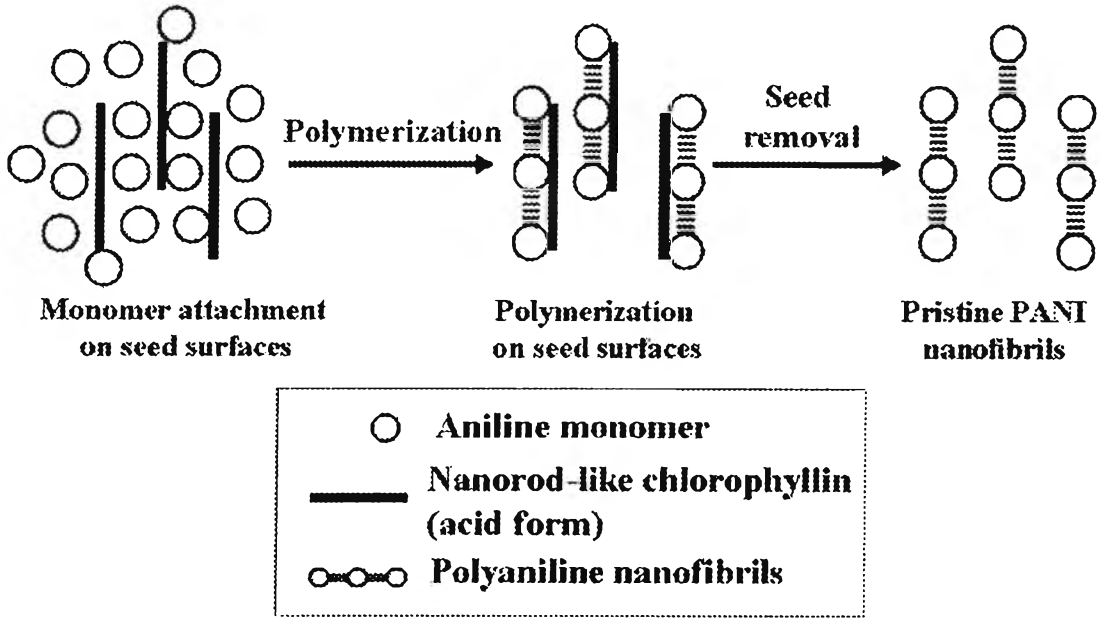

Schematic 4.2 Proposed mechanism of formation of the synthesized PANI nanofibrils based on adsorption of anilinium ion on chlorophyllin nanorod seed particles.

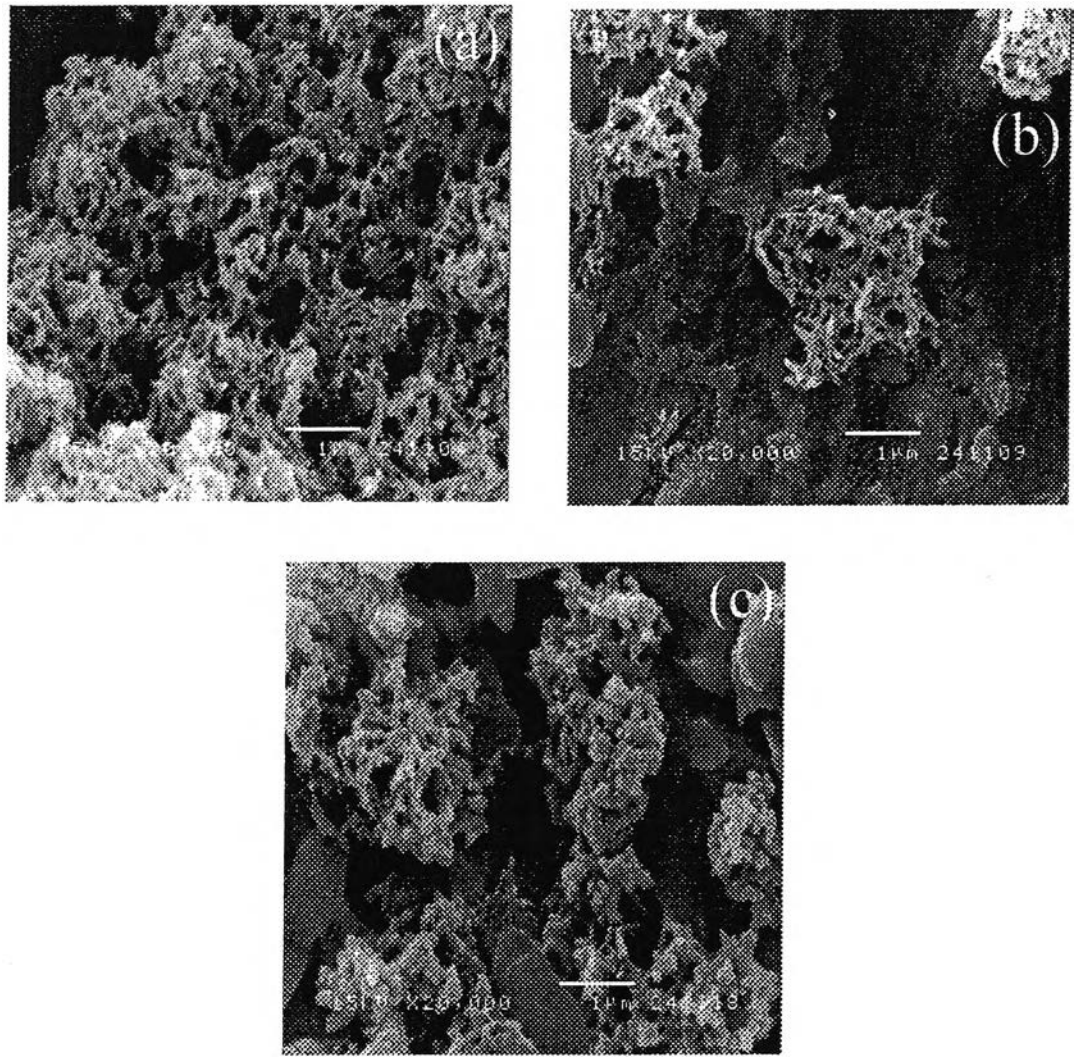

Figure 4.5 SEM images of PANI polymerized in the presence of 8.14×10^{-3} mole ratio of chlorophyllin to aniline monomer after washing with different solvents: a) acetone; b) 0.5 M NaOH; and c) distilled water.

4.4.4 Thermogravimetric Analysis (TGA)

TGA thermograms of the chlorophyllin seed and the distinct forms (PANI EB and PANI ES) of conventional PANI and PANI synthesized using seeding polymerization are shown in Figure 4.6. The acid form of chlorophyllin exhibits three discrete weight losses at approximately 80, 280, and 440°C, as shown in Figure 4.6a, which are attributed, respectively, to the evaporation of water, the elimination of the Cu^{II} ion, and the degradation of the porphyrin structure. Figure 4.6b, showing the TGA thermogram of the conventional PANI EB, indicates two discrete weight

losses appearing at approximately 80 and 500°C, which correspond to the loss of water and the degradation of PANI chains, respectively. Similar weight loss patterns were observed in the PANI EB nanofibrils synthesized in the presence of different chlorophyllin contents after washing with 0.5 M NaOH solution (data not shown). In contrast, for conventional PANI ES (Fig. 4.6c), three discrete weight losses are observed at approximately 80, 280, and 500°C owing to the loss of water, the elimination of dopant, and the degradation of PANI chains, respectively (Kan, Zhou, Zhang, Patel 2006; Chan, Teo, Khor, Lim. 1989; Neoh, Kang, Tan. 1990). Again, it was observed that there was no difference in weight loss pattern of the PANI ES nanofibrils synthesized in the presence of different chlorophyllin content after washing with acetone (Fig. 4.6d). This indicates that the addition of chlorophyllin causes only a change in morphology of the PANI products, and does not affect the thermal stability of the resulting PANI after removal of the chlorophyllin seed. Finally, Figure 4.6e shows the TGA thermogram of PANI nanofibrils without removal of the chlorophyllin seed. This thermogram reveals the weight loss characteristics of both PANI and chlorophyllin; specifically, the elimination of the Cu^{II} ion and the degradation of chlorophyllin at 280 and 440°C, respectively, and the degradation of PANI chains at 500°C.

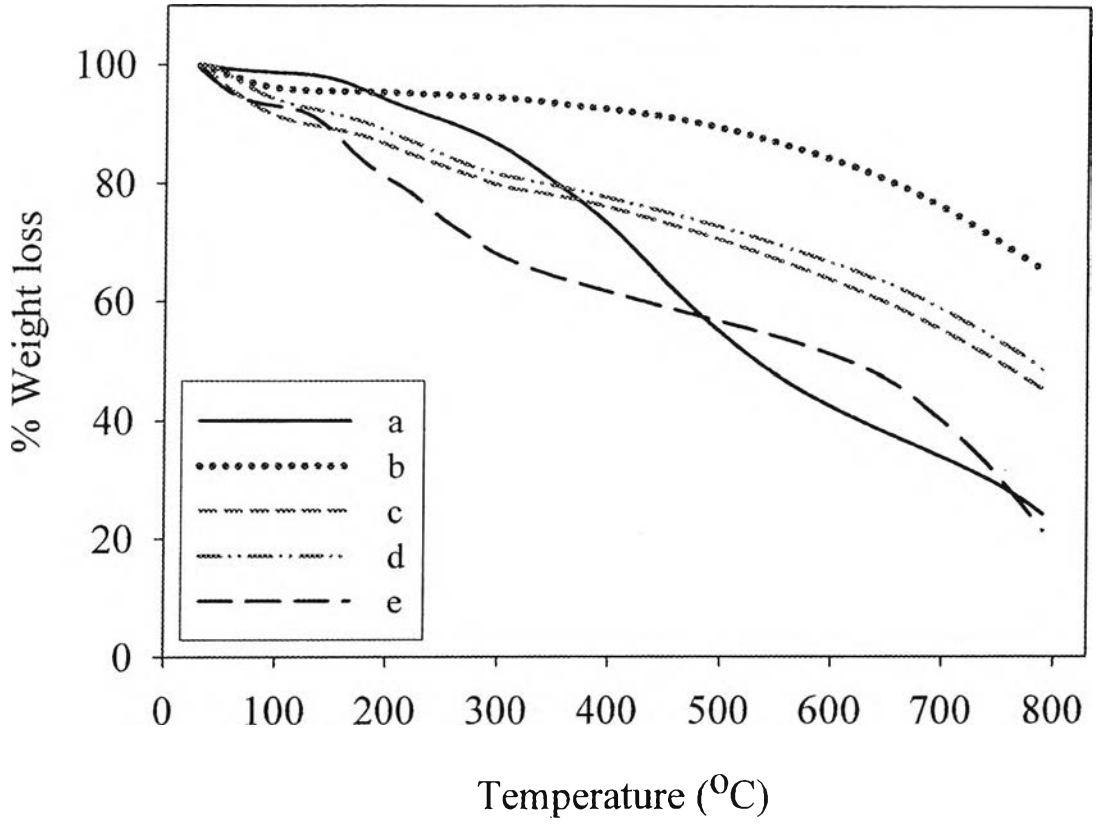

Figure 4.6 TGA thermograms of a) nanorod-like chlorophyllin (acid form); b) conventional PANI EB; c) conventional PANI ES; d) PANI ES polymerized in the presence of 4.07×10^{-2} mole ratio of chlorophyllin to aniline monomer after washing with acetone; and e) PANI ES polymerized in the presence of 4.07×10^{-2} mole ratio of chlorophyllin to aniline monomer without washing with acetone.

4.4.5 Wide Angle X-ray Diffraction (WAXD)

Figure 4.7 shows the X-ray diffraction patterns which were used to identify the crystalline structure of chlorophyllin and PANI synthesized in the presence of chlorophyllin seed. For the pure chlorophyllin (Fig. 4.7a), two broad diffraction peaks, centered approximately at $2\theta = 9°$ and $2\theta = 20°$, were observed, suggesting an amorphous structure. Similar to chlorophyllin, as shown in Figure 4.7d, the PANI EB nanofibrils obtained after washing with 0.5 M NaOH feature a small diffraction peak at $2\theta = 9°$ and a broad peak centered at $2\theta = 20°$, which likewise

indicates an amorphous structure for PANI EB. On doping the PANI EB with HCl, the structure of PANI EB rearranges to form PANI ES, which exhibits a highly-ordered structure with a highly π-conjugated system. This structural change was confirmed by the appearance of a more sharply defined diffraction pattern, characteristic of the semi-crystalline PANI ES, with an intense peak at $2\theta = 25°$ and weaker peaks at $2\theta = 9°$, 15°, 20°, and 26°, for PANI ES samples synthesized with different chlorophyllin contents (see, Figs. 4.7b and 4.7c), as well as for the PANI ES synthesized by the conventional method (data not shown). This further supports that the addition of chlorophyllin causes a change in morphology, but does not affect the crystalline structure of the resulting PANI nanofibrils.

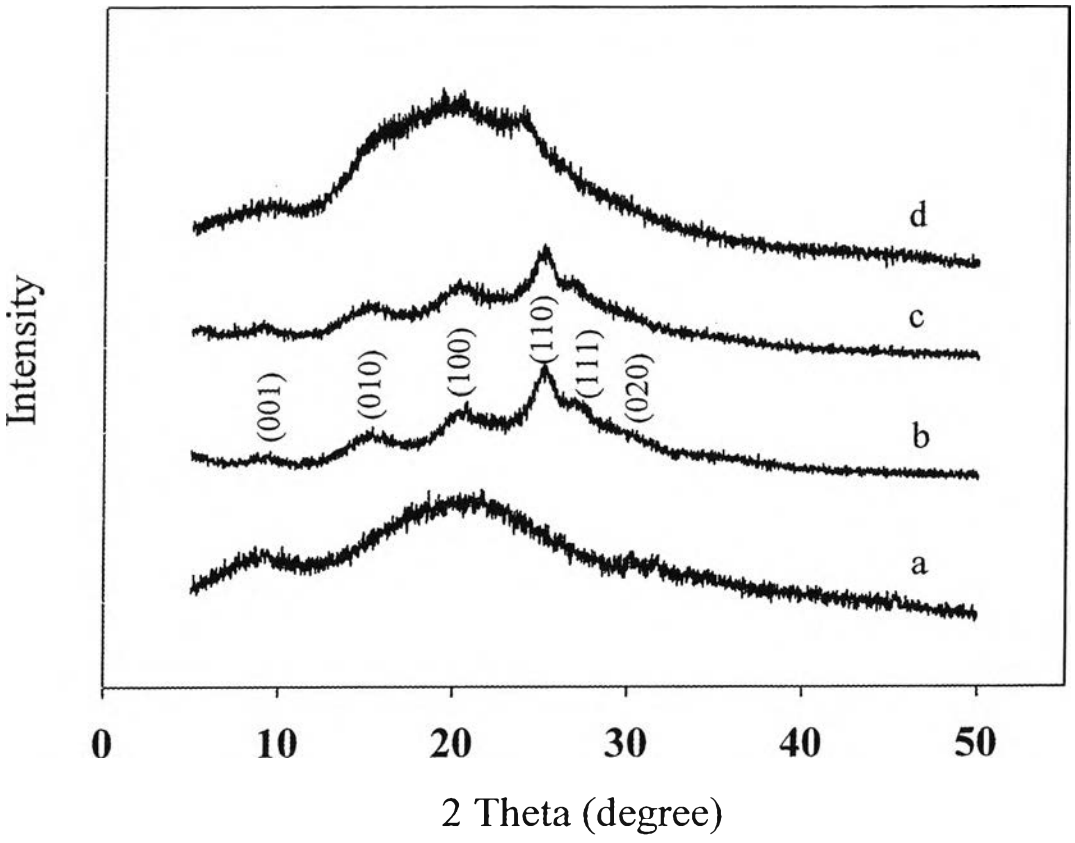

Figure 4.7 XRD patterns of a) chlorophyllin powder; PANI ES polymerized in the presence of b) 8.14×10^{-4} mole ratio of chlorophyllin to aniline monomer; c) 4.07×10^{-2} mole ratio of chlorophyllin to aniline monomer after washing with acetone; and d) PANI EB polymerized in the presence of 4.07×10^{-2} mole ratio of chlorophyllin to aniline monomer, after washing with 0.5 M NaOH.

4.4.6 Electrical Property

The electrical conductivities of the pressed PANI samples, in both undoped and doped states, synthesized in the presence of different chlorophyllin contents are listed in Table 4.1. It was observed that conventional PANI as well as PANI synthesized with different chlorophyllin contents, in the undoped state (PANI EB), each exhibits electrical conductivities of the order of 10^{-11} S/cm, confirming the insulating character of PANI EB. On the other hand, the electrical conductivities of the corresponding PANI synthesized in the doped state (PANI ES) were higher than those of PANI EB, by approximately 12 orders of magnitude. This reflects the highly π-conjugated system and the highly-ordered structure of PANI ES compared to PANI EB, as apparent in the XRD patterns of the PANI products (see Fig. 4.7). Moreover, the electrical conductivities of the PANI ES nanofibrils, using synthesized mole ratios of chlorophyllin to aniline monomer of 8.14×10^{-4}, 8.14×10^{-3}, and 1.63×10^{-2}, are each comparable to that of conventional PANI ES. This indicates that the change in morphology of the nanofibrillar PANI ES does not significantly influence the electrical conductivity of the pressed products. A similar result was reported previously by King *et al.*, who synthesized PANI nanofibers by two different polymerization methods; viz. interfacial polymerization and polymerization seeded using single-walled carbon nanotubes. These authors report that the overall conductivities of the as-synthesized PANI nanofibers were comparable to those prepared by the conventional method (King, Roussel 2005). On the other hand, Table 4.1 indicates that, when the chlorophyllin content is increased up to a mole ratio of 4.07×10^{-2}, the electrical conductivity of the synthesized PANI decreases. This is presumably an adverse effect of the residual chlorophyllin in the corresponding PANI ES product. Here, a word of caution is appropriate: the electrical conductivities reported in Table 1 were determined using pressed pellets and it is possible that the PANI nanofibrils may undergo a change in morphology, when compressed during the sample preparation. Thus, the measured conductivities may in fact reflect the bulk polymer property.

Table 4.1 Electrical conductivities of pelletized PANI samples

Sample*	Specific conductivity (S/cm)	
	Undoped state**	Doped state
Conventional PANI	$2.81\times10^{-11}\pm 1.12\times10^{-12}$	15.6 ± 0.32
PANI with 8.14×10^{-4} mole chlorophyllin/mole aniline	$2.81\times10^{-11}\pm 1.01\times10^{-12}$	18.3 ± 0.33
PANI with 8.14×10^{-3} mole chlorophyllin/mole aniline	$3.05\times10^{-11}\pm 6.75\times10^{-13}$	21.1 ± 1.02
PANI with 1.63×10^{-2} mole chlorophyllin/mole aniline	$3.18\times10^{-11}\pm 5.51\times10^{-13}$	12.3 ± 0.44
PANI with 4.07×10^{-2} mole chlorophyllin/mole aniline	$3.26\times10^{-11}\pm 1.95\times10^{-12}$	8.28 ± 0.28

* Samples were prepared by compression of PANI to form pellets.

** The synthesized PANI ES powder was immersed in 1 M NaOH (1 g of PANI ES : 50 g of 1 M NaOH) for 2 h.

4.5 Conclusion

Highly uniform PANI nanofibrils, with diameters in the range of 60–100 nm, were successfully synthesized via an *in-situ* seeding technique, using chlorophyllin nanorods as the *in-situ* seed. The mechanism of formation of the PANI nanofibrils is attributed to the directed polymerization of aniline monomer along the surfaces of the chlorophyllin seed. Pristine PANI nanofibrils were obtained after removing the chlorophyllin seed by washing with acetone or 0.5 M NaOH solution, resulting in the doped (PANI ES) and undoped (PANI EB) states of PANI, respectively. The morphology of the PANI was influenced by the concentration of chlorophyllin. PANI nanofibrils were obtained on addition of chlorophyllin mole ratios to aniline monomer of 8.14×10^{-4}, 8.14×10^{-3}, and 1.63×10^{-2}, whereas, at a mole ratio of 4.07×10^{-2}, extensive aggregation of PANI was observed. It was established, moreover, that the presence of the chlorophyllin seed causes a change in morphology

only, and does not influence the molecular structure of the resulting PANI (as confirmed by several characterization techniques, including UV-Visible spectroscopy, FTIR, TGA, and XRD). The electrical conductivities of the pressed PANI nanofibrils in both PANI EB and PANI ES states were comparable to those of the conventional PANI. While no significant differences in electrical conductivity were observed between the pressed conventional PANI and the pressed nanofibrillar PANI, we note that, due to the smaller size of the PANI nanofibrils compared to the conventional PANI, it is of interest to further investigate their dispersion and electrical conductivity behavior in other polymer matrixes. In this regard, the use of chlorophyllin, as an *in-situ* seed, which can be easily removed by washing with acetone or NaOH solution, appears to be a simple alternative approach to synthesize pristine PANI nanofibrils in bulk quantities.

4.6 Acknowledgements

The authors gratefully acknowledge the Thailand Research Fund (Royal Golden Jubilee Ph.D Scholarship), the National Nanotechnology Center, and the Conductive and Electroactive Polymers Research Unit, Chulalongkorn University, Thailand, for their financial support of this work. AMJ also wishes to acknowledge financial support from the National Science Foundation, Polymers Program, under grant no. DMR 0513010.

4.7 References

Ajay, AK. Divesh, N. and Srivastava. (2007) Microtubular conductometric biosensor for ethanol detection. Biosensors and Bioelectronics, 23, 281-284.

Aussawasathien, D. Dong, J.H. and Dai. L. (2005) Electrospun polymer nanofiber sensors. Synthetic Metals, 154, 37-40.

Bai, X. Li, X. Li, N. Zuo, Y. Wang, L. Li, J. and Qiu, S. (2007) Synthesis of cluster polyaniline nanorod via a binary oxidant system. Materials Science and Engineering C, 27, 695-699.

Banerjee, P. and Mandal, BM. (1995) Blends of HCl-doped polyaniline nanoparticles and poly(vinyl chloride) with extremely low percolation threshold — a morphology study. Synthetic Metals, 74, 257-261.

Chan, H.S.O. Teo, M.T.B. Khor, E. and Lim, C.N. Thermal analysis of conducting polymers part I: Thermogravimetry of acid-doped polyanilines. Journal of Thermal Analysis and Calorimetry, 35, (1989) 765-774.

Cheng, D. Ng, S. and Chan. H.S.O. (2005) Morphology of polyaniline nanoparticles synthesized in triblock copolymers micelles, Thin Solid Films, 477, 19-23.

Chiou, N.R. and Epstein. A.J. (2005) A Simple Approach to Control the Growth of Polyaniline Nanofibers. Synthetic Metals, 153, 69-72.

Cho, M.S. Park, S.Y. Hwang, J.Y. Cho, H.J. (2004) Synthesis and electrical properties of polymer composites with polyaniline nanoparticles. Materials Science and Engineering C, 24, 15-18.

Choi, HJ. Kim, TW. Cho, MS. Kim, SG. and Jhon, MS. (1997) Electrorheological characterization of polyaniline dispersions, European Polymer Journal, 33, 699-703.

Dhand, C. Singh, S.P. Arya, S.K. Datta, M. and Malhotra, B.D. (2007) Cholesterol biosensor based on electrophoretically deposited conducting polymer film derived from nano-structured polyaniline colloidal suspension. Analytica Chimica Acta, 602, 244-251.

Gu, D.W. Li, J.S. Li, J.L. Cai, Y.M. and Shen, L.J. (2005) Polyaniline thin films in situ polymerized under very high pressure. Synthetic Metals, 150, 175-179.

Guo, Y. and Zhou. Y. (2007) Polyaniline nanofibers fabricated by electrochemical polymerization: A mechanistic study. European Polymer Journal, 43, 2292-2297.

Gupta, Y. Hellgardt, K. and Wakeman, RJ. (2006) Enhanced permeability of polyaniline based nano-membranes for gas separation. Journal of Membrane Science, 282, 60-70.

Han, MG. Cho, SK. Oh, SG. and Im. SS. (2002) Preparation and characterization of polyaniline nanoparticles synthesized from DBSA micellar solution. Synthetic Metals, 126, 53-60.

He, H.X. Li, C.Z. and Tao, N.J. (2001) Conductance of polymer nanowires fabricated by a combined electrodeposition and mechanical break junction method. Applied Physics Letters, 78, 811-813.

He. Y. (2005) Interfacial synthesis and characterization of polyaniline nanofibers. Materials Science and Engineering B, 122, 76-79.

He, Y. (2005) Preparation of polyaniline microspheres with nanostructured surfaces by a solids-stabilized emulsion. Material Letter, 59, 2133-2136.

Huang, J. and Kaner, R.B. (2004) A General Chemical Route to Polyaniline Nanofibers Journal of the American Chemical Society, 126, 851-855.

Huang, J. Virji, S. Weiller, B.H. and Kaner, R.B. (2004) Nanostructured Polyaniline Sensors. Chemistry - A European Journal, 10, 1314-1319.

Jayanty, S. Prasad, G.K. Sreedhar, B. and Radhakrishnan, T.P. (2003) Polyelectrolyte templated polyaniline—film morphology and conductivity. Polymer, 44 7265-7270.

Jing, X. Wang, Y. Wu, D. and Qiang, J. (2007) Sonochemical synthesis of polyaniline nanofibers, Ultrasonics Sonochemistry, 14, 75-80.

Jing, X. Wang, Y. Wu, D. She, L. and Guo, Y. (2006) Polyaniline nanofibers prepared with ultrasonic irradiation. Journal of Polymer Science Part A: Polymer Chemistry, 44, 1014-1019.

Kahol, P.K. and Pinto, N.J. (2002) Electron paramagnetic resonance investigations of electrospun polyaniline fibers, Solid State Communications, 124, 195-197.

Kan, J. Zhou, S. Zhang, Y. and Patel, M. (2006) Synthesis and characterization of polyaniline nanoparticles in the presence of magnetic field and samarium chloride. European Polymer Journal, 42, 2004-2012.

Kim, B.J. Oh, S.G. Han, M.G. and Im, S.S. (2001) Synthesis and characterization of polyaniline nanoparticles in SDS micellar solutions, Synthetic Metals, 122 297-304.

King, R.C.Y. and Roussel, F. (2005) Morphological and electrical characteristics of polyaniline nanofibers. Synthetic Metals, 153, 337-340.

Li, M. Gou, Y. Wei, Y. MacDiarmid, A.G. and Lelkes, P.I. (2006) Electrospinning polyaniline-contained gelatin nanofibers for tissue engineering applications. Biomaterials, 27, 2705-2715.

Li, X. Zhao, Y. Zhuang, T. Wang, G. and Gu, O. (2007) Self-dispersible conducting polyaniline nanofibres synthesized in the presence of β-cyclodextrin. Colloids and Surfaces A, 295, 146-151.

Liu, F.J. Huang, L.M. Wen, T.C. and Gopalan, A. (2007) Large-area network of polyaniline nanowires supported platinum nanocatalysts for methanol oxidation Synthetic Metals, 157, 651-658.

Martin, CR. (1996) Membrane-Based Synthesis of Nanomaterials. Chemistry of Materials, 8, 1739-1746.

Mazur, M. Tagowska, M. Palys, B. and Jakowska, K. (2003) Template synthesis of polyaniline and poly(2-methoxyaniline) nanotubes: comparison of the formation mechanisms. Electro-chemistry Communications, 5, 403-407.

Neoh, K.G. Kang, E.T. and Tan. K.L. (1990) Thermal degradation of leucoemeraldine, emeraldine base and their complexes. Thermochimica Acta, 171, 279-291.

Park, SJ. Park, SY. Cho, MS. Choi, HJ. and Jhon, MS. (2005) Synthesis and electrorhelogy of multi-walled carbon nanotube/polyaniline nanoparticles, Synthetic Metals, 152, 337-340.

Pillalamarri, S.K. Blum, F.D. Tokuhiro, A.T. Story, J.G. and Bertino, M.F. (2005) Radiolytic synthesis of polyaniline nanofibers: a new templateless pathway. Chemistry of Materials, 17, 227-229.

Sadek, A.Z. Wlodarski, W. Kalantar-Zadeh, K. Baker, C. and Kaner, R.B. (2007) Doped and dedoped polyaniline nanofiber based

conductometric hydrogen gas sensors. Sensors and Actuator A, 139, 53-57.

Stejskal, J. and Sapurina, I. (2004) On the origin of colloidal particles in the dispersion polymerization of aniline. Journal of Colloid and Interface Science, 274, 489-495.

Stejskal, J. Sapurina, I. Trchova, M. Konyushenko, E.N. and Holler, P. (2006) The genesis of polyaniline nanotubes. Polymer, 47, 8253-8262.

Sun, Q. Park, MC. and Deng. Y. (2007) Dendritic superstructure formation of polyaniline prepared using a water-soluble polyelectrolyte copolymer as the support matrix. Material Letter, 61, 3052-3055.

Teoh, G.L. Liew, K.Y. and Mahmood W.A.K. (2007) Preparation of polyaniline-Al_2O_3 composites nanofibers with controllable conductivity. Material Letter, 61, 4947-4949.

Virji, S. Huang, J. Kaner, R.B. and Weiller, B.H. (2004) Polyaniline Nanofiber Gas Sensors: Examination of Response Mechanisms. Nano Letter, 4, 491-496.

Wang, F. Xu, X. Gong, J. Luo, Y. Hou, Y. Zheng, X. and Qu, L. (2005) Polyaniline microrods synthesized by a polyoxometalates/poly(vinyl alcohol) microfibers template. Materials Letters, 59, 3982-3985.

Wang, F. Yang, R. Gong, J. Sui, C. Luo, Y. and Qu, L. (2006) Synthesis and characterization of polyaniline microfibers by utilizing $H_4SiW_{12}O_{40}$/polyacrylamide microfibers seeding template method. European Polymer Journal, 42, 2108-2113.

Wang, Y. Jing, X. and Kong, J. (2007) Polyaniline nanofibers prepared with hydrogen peroxide as oxidant. Synthetic Metals, 157, 269-275.

Wang, Y. and Jing, X. (2007) Transparent conductive thin films based on polyaniline nanofibers. Materials Science and Engineering B, 138, 95-100.

Wang, Y. and Jing, X. (2008) Formation of polyaniline nanofibers: a morphological study. Journal of Physical Chemistry B, 112, 1157-1162.

Wei, D. Kvarnstrom, C. Lindfors, T. and Ivaska, A. (2006) Polyaniline nanotubules obtained in room-temperature ionic liquids, Electrochemistry Communications, 8, 1563-1566.

Werake, LK. Story, JG. Bertino, MF. Pillalamarri, SK. and Blum, FD. (2005) Photolithographic synthesis of polyaniline nanofibres. Nanotechnology, 16 2833-2837.

Wu, CG. and Bein, T. (1994) Conducting polyaniline filaments in a mesoporous channel host. Science, 264, 1757-1759.

Xian, Y. Liu, F. Feng, L. Wu, F. Wang, L. and Jin, L. (2007) Nanoelectrode ensembles based on conductive polyaniline/poly(acrylic acid) using porous sol–gel films as template. Electrochemistry Communications, 9, 773-780.

Xing, S. Zhao, C. Jing, S. and Wang, Z. (2006) Morphology and conductivity of polyaniline nanofibers prepared by 'seeding' polymerization, Polymer, 47, 2305-2313.

Xiong, S. Wang, Q. and Xia. H. (2004) Preparation of polyaniline nanotubes array based on anodic aluminum oxide template. Materials Research Bulletin, 39, 1569-1580.

Yang, X. Zhao, T. Yu, Y. and Wei, Y. (2004) Synthesis of conductive polyaniline/epoxy resin composites: doping of the interpenetrating network. Synthetic Metals, 142, 57-61.

Zhang, D. and Wang. Y. (2006) Synthesis and applications of one-dimensional nano-structured polyaniline: An overview. Materials Science and Engineering B, 134, 9-19.

Zhang, X. Goux, WJ. and Manohar, SK. (2004) Synthesis of polyaniline nanofibers by nanofiber seeding. Journal of the American Chemical Society, 126, 4502-4503.

Zhang, X. Kolla, H.S. Wang, X. Raja, K. and Manohar, S.K. (2006) Fibrillar growth in polyaniline. Advanced Functional Materials, 16, 1145-1152.

Zhang, X. and Manohar, S.K. (2004) Bulk synthesis of polypyrrole nanofibers by a seeding approach. Journal of the American Chemical Society, 126, 12714-12715.

Zhang, Z. and Wan, M. (2002) Composite films of nanostructured polyaniline with poly(vinyl alcohol). Synthetic Metals, 128, 83-89.

Zhu, J. and Jiang, W. (2007) Fabrication of conductive metallized nanostructures from self-assembled amphiphilic triblock copolymer templates: Nanospheres, nanowires, nanorings. Material Chemistry and Physics, 101, 56-62.

Zhu, N. Chang, Z. He, P. and Fang, Y. (2006) Electrochemically fabricated polyaniline nanowire-modified electrode for voltammetric detection of DNA hybridization, Electrochimica Acta, 51, 3758-3762.